Trinuclear NiII-LnIII-NiII Complexes

Subjects:
Contributor: Catherine Raptopoulou

This entry summarizes the structural characteristics and magnetic properties of trinuclear complexes containing the NiII-LnIII-NiII moiety. The ligands used are mainly polydentate Schiff base ligands and reduced Schiff base ligands and, in some cases, oximato, β-diketonato, pyridyl ketone ligands and others. The compounds reported are restricted to those containing one, two and three oxygen atoms as bridges between the metal ions; examples of carboxylato and oximato bridging are also included due to structural similarity. The magnetic properties of the complexes range from ferro- to antiferromagnetic depending on the nature of the lanthanide ion.

Keywords: heterometallic complexes ; trinuclear moiety ; nickel(II) ; lanthanide(III) ions ; crystal structures ; magnetic properties

1. Tripodal Polydentate Schiff Base Ligands and Reduced Schiff Base Ligands

A new phosphorus-supported ligand H_3L^1 = (S)P[M(Me)N=CH-C_6H_3-2-OH-3-OMe]$_3$ (Scheme 1), prepared by the condensation of (S)P[M(Me)NH_2]$_3$ and *o*-vanillin, was used to synthesize the trinuclear isomorphous complexes [(NiL^1)$_2$Ln](ClO_4) (Ln = La-Er, except Pm, **1**–**11**)[1]. The cation consists of three nearly linear metal ions, two terminal Ni^{II} and one Ln^{III} in the center (Figure 1). Each of the terminal Ni^{II} is bound to the three imino nitrogen and the three phenolato oxygen atoms of one $(L^1)^{3-}$, thus describing an in situ formed $[NiL^1]^-$ metalloligand. Two such metalloligands are bound to the central Ln^{III} ion through the phenolato and methoxy oxygen atoms of the two ligands, describing a distorted icosahedral. The Ln-O bond distances show a gradual reduction in accordance with lanthanide contraction. The Ni_2Gd (**7**), Ni_2Dy (**9**) and Ni_2Er (**11**) complexes display ferromagnetic interactions between the metal ions. The magnetic susceptibility measurements of **7** were interpreted by using the spin Hamiltonian where $S_{Ni1} = S_{Ni2} = 1$ and $S_{Gd} = 7/2$. The best set of parameters obtained using this model is J/k_B = +0.375 cm^{-1} and g = 2.04. The magnetization measurements of **7** as a function of the field show relatively rapid saturation of the magnetization at high fields and agree with an S = 11/2 spin ground state. Ac susceptibility measurements of the Ni_2Dy complex (**9**) as a function of the temperature at different frequencies and also as a function of the frequency at different temperatures under zero and 3500 Oe dc field showed that **9** exhibits slow relaxation of the magnetization and observation of field induced single-molecule magnet behavior. The data were fitted to an Arrhenius law in order to estimate the energy gap of 10.8 K and pre-exponential factor $\tau_0 = 2.3 \times 10^{-5}$ s. The value of 10.8 K is in the range observed for similar complexes, however the value of τ_0 is much larger than expected suggesting that the quantum pathway of relaxation is only partially suppressed by the applied field of 3500 Oe and hence that the energy gap of the thermally activated relaxation should be higher than 10.8 K. In any case, the magnetic study of **9** suggests SMM behavior generated by the high spin ground state of the complex and the magnetic anisotropy of the Dy^{III} ion. All other complexes behave as simple paramagnetic systems. DFT calculations on the Ni_2Gd (**7**) and Ni_2La (**1**) complexes revealed good agreement between the experimental and computed J values, confirmed the ferro- and antiferromagnetic nature of the J_{NiGd} and J_{NiNi} interactions, respectively and gave information on the spin densities of the metal ions and bridging oxygen atoms[2].

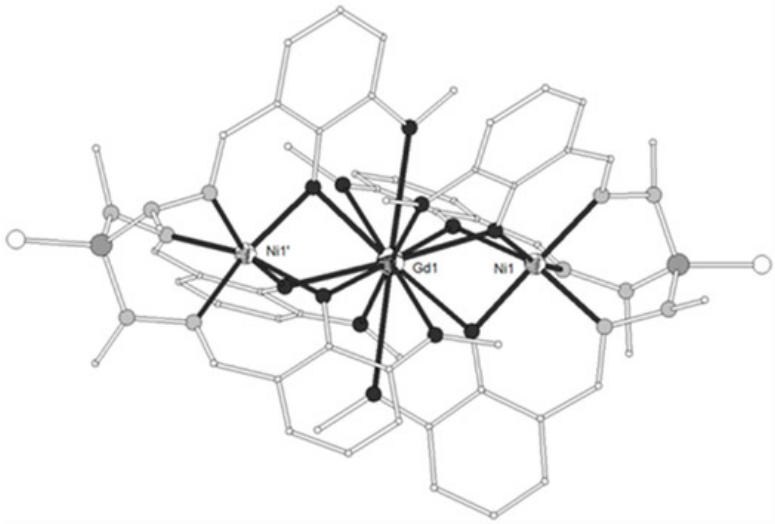

Figure 1. The molecular structure of the cation $[(NiL^1)_2Gd]^+$ in complex **7**. Primed atoms are generated by symmetry: (') = -*x*, *y*, 1-*z*. Color code: Gd large octant, Ni small octant, N light grey, O dark grey, C open small, P grey large, S open large[1].

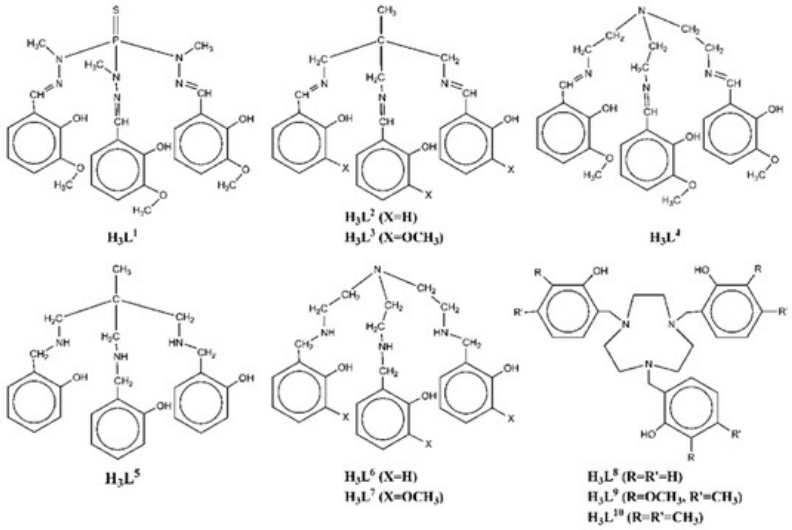

Scheme 1. The tripodal polydentate Schiff base and reduced Schiff base ligands used in the Ni_2Ln complexes **1**–**70**.

The tripodal hexadentate Schiff base-phenolate ligand H_3L^2 = 2,2'-((1*E*)-((2-(((*E*)-(2-hydroxybenzylidene)amino)methyl)-2-methylpropane-1,3-diyl)bis(azanylylidene))bis(methanylylid ene))diphenol (Scheme 1) was used to synthesize the neutral trinuclear complexes $[(NiL^2)_2Ln(NO_3)]$ (Ln^{III} = Gd, Eu, Tb, Dy, **12**–1**5**)[3][4] which show a Ni-Ln-Ni angle of ca. 140° (Figure 2). All four complexes have similar structures with the two terminal Ni^{II} ions coordinated to the three imino nitrogen and three phenolato oxygen atoms of one $(L^2)^{3-}$. The coordination geometry of each Ni^{II} ion is distorted from a regular octahedron toward a trigonal prism with trigonal twist angle f ~45° (trigonal prism = 0°, octahedron = 60°). The central Ln^{III} ion is bound to the phenolato oxygen atoms of the ligands and to chelate nitrato ligand. All complexes exhibit 3D structures due to intermolecular π-π and CH-π interactions between neighboring molecules. The magnetic data for the Ni_2Gd (**12**) complex are consistent with ferromagnetic coupling between the metal ions giving rise to a ground state with spin S = 11/2. The best-fit parameters to the experimental magnetic susceptibility data of **12** were g = 2.24, J(Ni-Gd) = +0.19 cm^{-1} and D = +2.1 cm^{-1}. A ferromagnetic interaction is also suggested for the Ni_2Tb (**14**) and Ni_2Dy (**15**) complexes.

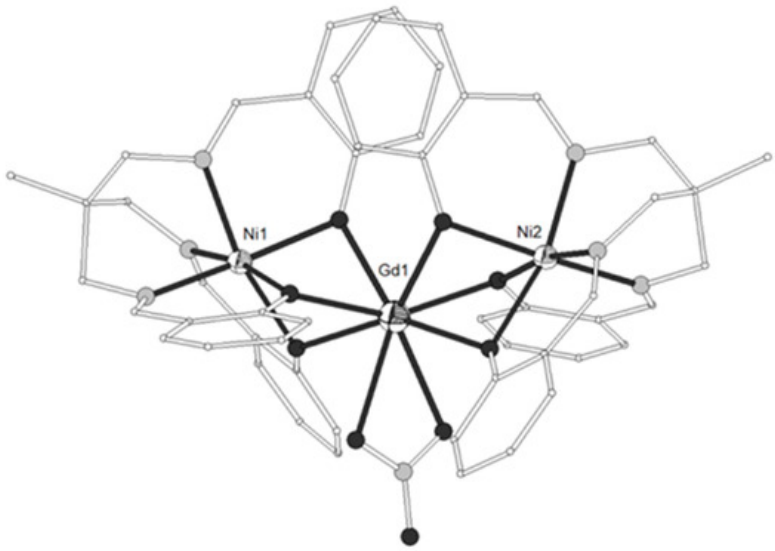

Figure 2. The molecular structure of complex $[(NiL^2)_2Gd(NO_3)]$ (**12**). Color code: Gd large octant, Ni small octant, N light grey, O dark grey, C open small[3].

The complex $[(NiL^3)_2Gd](NO_3)$ (**16**) (H_3L^3 = 6,6'-((1*E*)-((2-(((*E*)-(2-hydroxy-3-methoxybenzylidene)amino)methyl)-2-methylpropane-1,3-diyl)bis(azanylylidene))bis(methanylylid ene))bis(2-methoxyphenol), Scheme 1) contains also two $[NiL^3]^-$ metalloligands bound to a Gd^{III} ion in an almost linear arrangement (~178°)[5]. The asymmetric unit contains two different cationic entities, the first one possesses two slightly different Ni^{II} environments, while the second one is symmetry-related through the Gd^{III} ion. The coordination geometry around each Ni^{II} ion is distorted octahedral with N_3O_3 chromophore. The Gd^{III} ion is coordinated to twelve oxygen atoms, deprotonated phenoxo oxygens and neutral methoxy oxygens. The magnetic susceptibility data were interpreted in terms of the spin Hamiltonian considering two equivalent Ni1-Gd and Ni2-Gd exchange interactions *J* and identical ZFS terms *D*. The best-fit parameters are J_{NiGd} = 0.91 cm^{-1}, *g* = 1.98 and *D* = 4.5 cm^{-1}. The magnetization measurements at 2 K in the range 0–5 T were satisfactorily simulated with this set of parameters and confirmed an S = 11/2 ground state due to ferromagnetic coupling between the metal ions.

The tripodal ligand H_3L^4 = 6,6',6''-((1*E*,1'*E*)-((nitrilotris(ethane-2,1-diyl))tris (azanylylidene)) tris(methanylylidene))tris(2-methoxyphenol) (Scheme 1) gave four heterometallic complexes, $[(NiL^4)_2Ln](NO_3)$ (Ln^{III} = Gd, Tb, Dy, **17**–**19**) and $[(NiL^4)_2Dy](ClO_4)$ (**20**) which contain linear Ni-Ln-Ni moieties (Figure 3)[6]. The Gd^{III} ion exhibits rare seven-coordination to six bridging phenoxo oxygen atoms and one methoxy oxygen atom from one of the $(L^4)^{3-}$ ligands and can be considered as an intermediate between the capped trigonal prism (CTPR-7, C_{2v}) and the capped octahedron (CTPR-7, C_{3v}). The Ln^{III} ions in the remaining three complexes exhibit rare six-coordination which can be described as quasi trigonal antiprism (intermediate between octahedron OC-6, O_h and trigonal prism TPR-6 D_{3h}). The magnetic susceptibility measurements of **17** were interpreted by using the spin Hamiltonian and gave the best-fit parameters *g* = 2.04, *J* = 0.64 cm^{-1} and *zJ'* = 0.009 cm^{-1} (*R* = 6.99 × 10^{-3}). The magnetization at 1.8 K increases upon increasing the magnetic field and reaches a value of 11.87 *Nb* at 7 T consistent with an *S* = 11/2 ground spin state. The magnetic study of **18**–**20** is consistent with ferromagnetic coupling between the metal ions. Ac susceptibility measurements of **18**–**20** between 1.8–10.0 K and frequencies 3-969 Hz under zero dc field showed temperature- and frequency-dependent out-of-phase peaks for **19** and **20** suggesting SMM behavior. The relaxation time derived from the χ'' peaks follows the Arrhenius law $\tau = \tau_0 \exp(\Delta/k_BT)$ with effective energy barriers of 14.17 K (τ_0 = 1.09 × 10^{-6} s) for **19** and 11.13 K (τ_0 = 6.72 × 10^{-6} s) for **20** under zero dc field. Complexes **19** and **20** constitute rare examples of SMMs containing six-coordinate Dy^{III} ions.

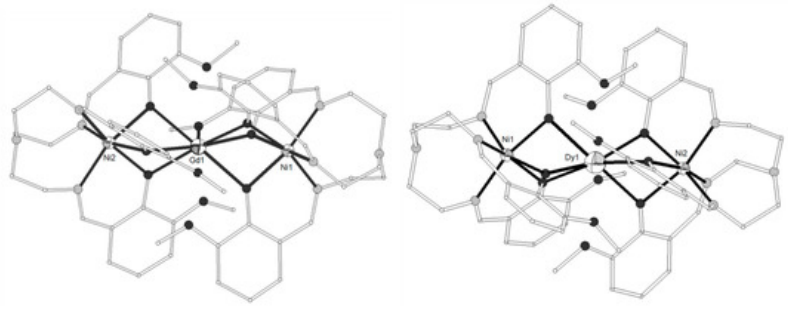

Figure 3. The molecular structures of the cations $[(NiL^4)_2Gd]^+$ (**17**, left) and $[(NiL^4)_2Dy]^+$ (**20**, right). Color code as in Figure 2[6].

The tripodal hexadentate amine phenol ligand H_3L^5 = 2,2'-(((2-(((2-hydroxybenzyl)amino)methyl)-2-methylpropane-1,3-diyl)bis(azanediyl))bis(methylen e))diphenol (Scheme 1), which is the reduced form of ligand H_3L^2, gave a series of isostructural complexes $[(NiL^5)_2Ln(solv)_x)](ClO_4)$ (Ln^{III} = La, Pr, Nd, Gd, Dy, Ho, Er, Yb; **21**–**28**; x = 2, $H_2O/(MeOH)_{0.5}/(EtOH)_{0.5}$ in Ni_2La, **21**; x = 2, H_2O/MeOH in Ni_2Dy, **25**; x = 1, H_2O in Ni_2Yb, **28**)[7]. The complexes consist of two $[NiL^5]^-$ metalloligands bound around the Ln^{III} ions with bent Ni-Ln-Ni moiety. The La^{III} ion in **21** is eight-coordinate to two $(L^5)^{3-}$ ligands which are tridentate with respect to the La^{III} ion and hexadentate with respect to one Ni^{II} ion. Two solvate molecules complete the coordination of the La^{III} ion which is described as a D_{4d} square antiprism distorted toward a C_{2v} bicapped octahedron. The Dy^{III} ion is seven-coordinate to two $[NiL^5]^-$ metalloligands, one bidentate and one tridentate and to two solvate molecules in a capped trigonal prismatic geometry. The Yb^{III} ion is six-coordinate to two $[NiL^5]^-$ metalloligands with a distorted octahedral geometry. The magnetic studies indicated that antiferromagnetic exchange coupling between the Ni^{II} and Ln^{III} ions increases with decreasing size of Ln^{III}.

The tripodal hexadentate amine phenol ligand H_3L^6 = 2,2',2''-(((nitrilotris(ethane-2,1-diyl))tris(azanediyl))tris(methylene))triphenol (Scheme 1) gave two series of isostructural complexes, $[(NiL^6)_2Ln(MeOH)](NO_3)$ (all Ln^{III} except Ce and Pm, **29**–**41**) and $[(NiL^6)_2Ln(MeOH)](ClO_4)$ (Ln^{III} = La, Pr, Nd, Sm, Gd, Dy, Ho, Er, **42**–**49**), which contain a bent Ni-Ln-Ni moiety with angles in the range ~139–144°[8][9]. In all structurally characterized complexes, the Ln^{III} ion is seven-coordinate being bicapped by two tridentate $[NiL^6]^-$ metalloligands and a methanol molecule in flattened pentagonal bipyramidal geometry. Each Ni^{II} ion is encapsulated by a full deprotonated ligand via four amine and two phenolato functions in approximately octahedral geometry. It is recognized that the coordination number of Ln^{III} ions tends to decrease with increased atomic number, that is, as the ionic radius decreases. However, in the present case, the coordination number and geometry of the Ln^{III} ions do not change along the entire Ln series plus La^{III}. Magnetic studies indicated that ferromagnetic exchange occurs in the case of Ni_2Ln with Ln^{III} = Gd, Tb, Dy, Ho, Er.

The congener ligand H_3L^7 = 6,6',6''-(((nitrilotris(ethane-2,1-diyl))tris(azane diyl))tris(methyl ene))tris(2-methoxyphenol) (Scheme 1) gave two isomorphous complexes $[(NiL^7)_2Ln)](ClO_4)$ (Ln^{III} = Gd, Dy, **50**–**51**) which contain a bent Ni-Ln-Ni moiety with angle ~113°[10]. The three metal ions are arranged in an isosceles triangle manner (Figure 4). The two terminal Ni^{II} ions are coordinated to four amine and two phenolate groups, whereas the central Ln^{III} ion is eight-coordinated to six bridging phenolato oxygen atoms and two methoxy oxygen atoms from the ligands presenting distorted dodecahedral geometry. The magnetic studies showed that both complexes exhibit ferromagnetic coupling between the metal ions. The magnetic susceptibility data of **50** were analyzed on the basis of the spin Hamiltonian (J' is assumed to be zero due to large distance between the Ni^{II} ions) and gave J/k = 1.02 cm^{-1} and g = 2.01. At 2 K, the magnetization is 11.04 $N\beta$ at 5 T which agrees with the saturation value of 11.94 $N\beta$ expected for an S = 11/2 system, confirming the ferromagnetic interaction between the Ni^{II} and Gd^{III} ions. The magnetization at 5 T for **51** is 12.65 $N\beta$ and is larger than the theoretical value of 12 $N\beta$ due to the presence of the anisotropic Dy^{III} ion. The Ni_2Dy complex **51** exhibited very weak field-induced slow relaxation of magnetization.

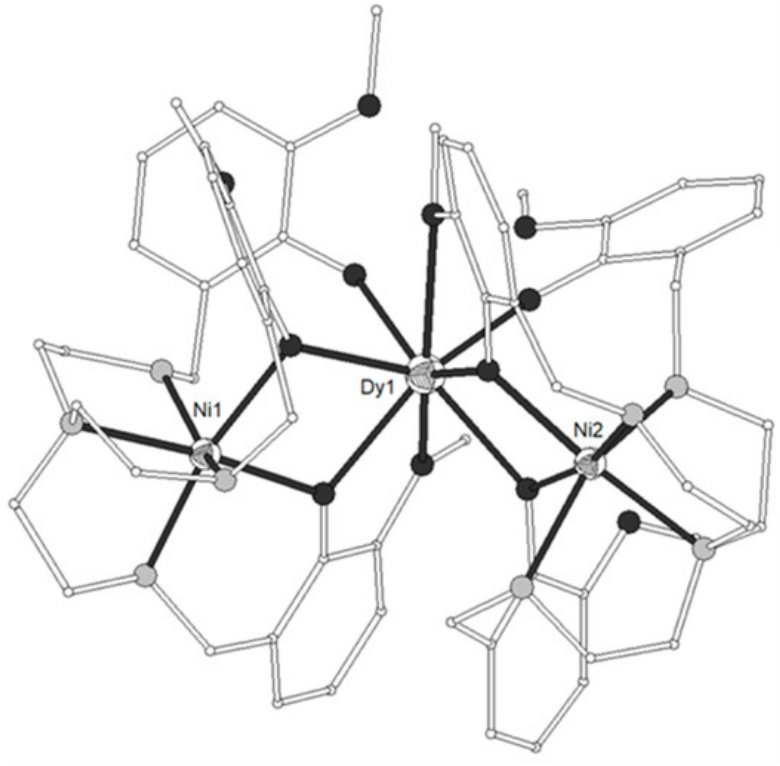

Figure 4. The molecular structure of the cation $[(NiL^{7})_2Dy)]^+$ in complex **51**. Color code as in Figure 2[10].

The ligand H_3L^8 = 2,2',2''-((1,4,7-triazonane-1,4,7-triyl)tris(methylene))triphenol (Scheme 1) gave the trinuclear complexes $[(NiL^8)_2Ln(MeCN)_2](ClO_4)$ (Ln^{III} = La, Nd, Gd, Dy, Yb, **52**–**55**) and $[(NiL^8)_2Yb](ClO_4)$ (**56**)[11]. The Gd^{III} ion in **54** is eight-coordinate in square antiprism distorted to C_{2v} bicapped trigonal prism geometry, bicapped by two deprotonated tridentate $(NiL^8)^-$ metalloligands (Figure 5). Each Ni^{II} is distorted octahedral in N_3O_3 coordination. The Ni-Gd-Ni angle is ~142°. The Yb^{III} ion in **56** is six-coordinated by six bridging phenolate oxygens (Figure 8). The decrease of the coordination number with increasing atomic number is common in Ln^{III} complexes. The complex is linear with Ni-Yb-Ni angle ~176°. Magnetic studies indicated ferromagnetic interactions for Ln^{III} = Gd, Dy, Yb and antiferromagnetic coupling for Ln^{III} = Nd.

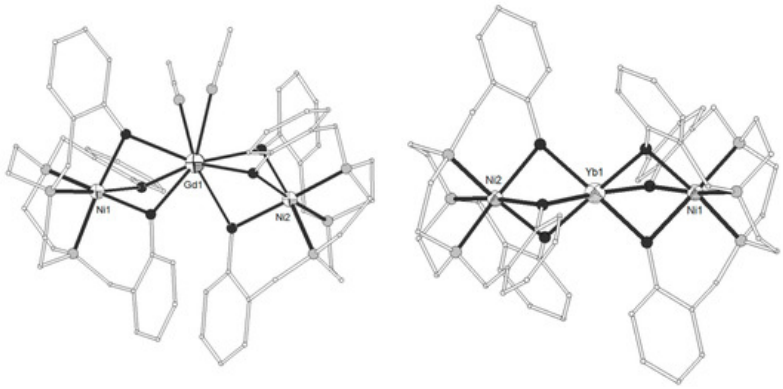

Figure 5. The molecular structures of the cations $[(NiL^8)_2Gd(MeCN)_2]^+$ **54**, (**left**) and $[(NiL^8)_2Yb]^+$ **56**, (**right**). Color code as in Figure 2[11].

The ligand H_3L^9 = 6,6',6''-((1,4,7-triazonane-1,4,7-triyl)tris(methylene))tris(2-methoxy-3-methylphenol) (Scheme 1) gave a series of 13 linear trinuclear complexes $[(NiL^9)_2Ln(solv)_x](ClO_4)$ (Ln^{III} = Y, La, Ce-Lu except Pr, Pm, Yb; x = 1, H_2O in Ni_2Sm, Ni_2Eu, Ni_2Tb; x = 0 in all other complexes, **57**–**69**)[12]. For complexes with Ln^{III} = Sm, Eu, Tb, the central lanthanide is seven-coordinate showing monocapped trigonal prismatic geometry (Figure S4). For the rest of the complexes, the central lanthanide as well as the terminal Ni^{II} ions are six-coordinate with coordination geometry between trigonal antiprism and trigonal prism and distorted octahedral, respectively. The Ni-Ln-Ni angles are in the range 165–179°. For **57**, **58** and **69** the $\chi_M T$ at 300 K is 2.48 cm^3Kmol^{-1}, 2.33 cm^3Kmol^{-1} and 2.76 cm^3Kmol^{-1}, higher than the theoretically expected value of 2.0 cm^3Kmol^{-1} because the diamagnetic Ln^{III} ions may induce small geometric variations and different ligand fields at the Ni^{II} ions, thus affecting the magnetic properties of the three complexes. The reduced magnetization for **57** and **69** shows a splitting of the isofield lines, which indicates a zero-field splitting. The best fit leads to $J_{Ni\text{-}Ni}$ = -0.294 cm^{-1}, g_{Ni} = 2.09, D_{Ni} = 1.933 cm^{-1} and E/D = 0.154 for **57** and $J_{Ni\text{-}Ni}$ = -0.129 cm^{-1}, g_{Ni} = 2.18, D_{Ni} = 2.838 cm^{-1} and E/D = 0.468 for **69**. The fit of the magnetic data of the Ni_2Gd complex **63** gave $J_{Ni\text{-}Ni}$ = -0.377 cm^{-1}, $J_{Gd\text{-}Ni}$ = -0.009 cm^{-1}, g_{Ni} = 2.102, g_{Gd} = 1.974 and χ^{TIP} = 0.003 cm^3Kmol^{-1}. Paramagnetic nuclear magnetic resonance (NMR) spectroscopy showed that in solution all complexes are isostructural showing the expected D_3 symmetry for all metal ions being six-coordinate. These complexes have small magnetic anisotropies and the NMR data agree with the solid state SQUID measurements.

The ligand H_3L^{10} = 6,6',6''-((1,4,7-triazonane-1,4,7-triyl)tris(methylene))tris(2,3-dimethylphenol) (Scheme 1) was used to prepare the linear complex $[(NiL^{10})_2Tb](ClO_4)$ (**70**)[13]. Each Ni^{II} ion is coordinated by three nitrogen and three phenolate oxygen atoms in octahedral geometry and the Tb^{III} ion is bound to six phenolate oxygen atoms in octahedral geometry. The magnetic studies revealed ferromagnetic interactions between the adjacent Ni^{II} and Tb^{III} ions.

2. Other Schiff Base Ligands

The Schiff base ligand HL^{11} = (*Z*)-2-methoxy-6-((phenylimino)methyl)phenol (Scheme 2) derived from the condensation of *o*-vanillin with aniline, gave the linear trinuclear complexes $[(NiL^{11}{}_3)_2Ln](NO_3)$ (Ln^{III} = La, Pr, Gd, Tb, **71**–**74**)[14][15] which contain two terminal Ni^{II} ions in octahedral N_3O_3 coordination and a central Ln^{III} ion bound to six phenolato and six methoxy oxygen atoms from six $(L^{11})^-$ ligands. The central Ln^{III} ion sits on inversion center and displays distorted icosahedron geometry (Figure 6). The Ni_2Gd complex **73** displays ferromagnetic coupling giving a ground spin state value of S = 11/2. Simultaneous fitting to $\chi_M T(T)$ and isothermal $M(H)$ plots by using the spin Hamiltonian and considering a single unique Ni-Gd interaction J_1, gave J_1 = +0.54 cm^{-1} with fixed g = 2.01. Q-band EPR spectra of polycrystalline **73** at 5 K can be reproduced by a model with S = 11/2 and ZFS parameters D = -0.135 cm^{-1}, E/D = 0.004 with g = 2.05. The magnetocaloric efficiency of the Ni_2Gd cluster **73** was studied for the first time for a linear Ni_2Gd cluster, via heat capacity and isothermal magnetization measurements which revealed a value of 13.74 $Jkg^{-1}K^{-1}$ for the magnetic entropy change

at 4 K and ΔH = 7 T. Weak ferromagnetic exchange between the Ni^{II} ions is found in the Ni_2La complex **71**. The experimental data were fitted by considering the spin Hamiltonian considering the zero-field splitting parameter D and gave J = +0.46 cm^{-1}, g = 2.245, D = +4.91 cm^{-1}. Dc magnetic susceptibility measurements revealed that the Ni^{II} ions are coupled ferromagnetically with the Tb^{III} ion in **74** and antiferromagnetically with the Pr^{III} ion in **72**. Ac susceptibility measurements performed on the Ni_2Tb complex **74** under zero dc field and under H = 0.5 T revealed the onset of frequency dependent χ''_M signals indicating the possibility of SMM behavior. The absence of clear maxima in the $\chi''_M(T)$ plots down to 2 K indicates fast magnetic relaxation or fast QTM or perhaps both.

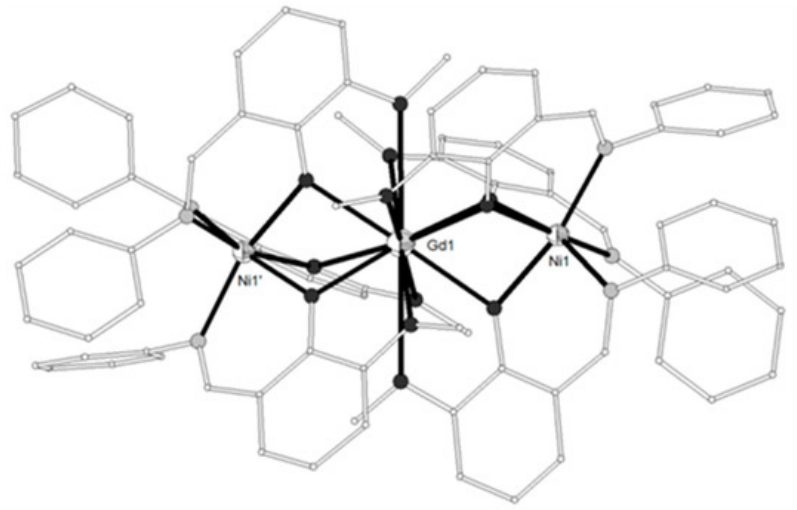

Figure 6. The molecular structure of the cation $[(NiL^{11}_3)_2Gd]^+$ in complex **73**. Primed atoms are generated by symmetry (') 1-x, y, 0.5-z. Color code as in Figure 2[14].

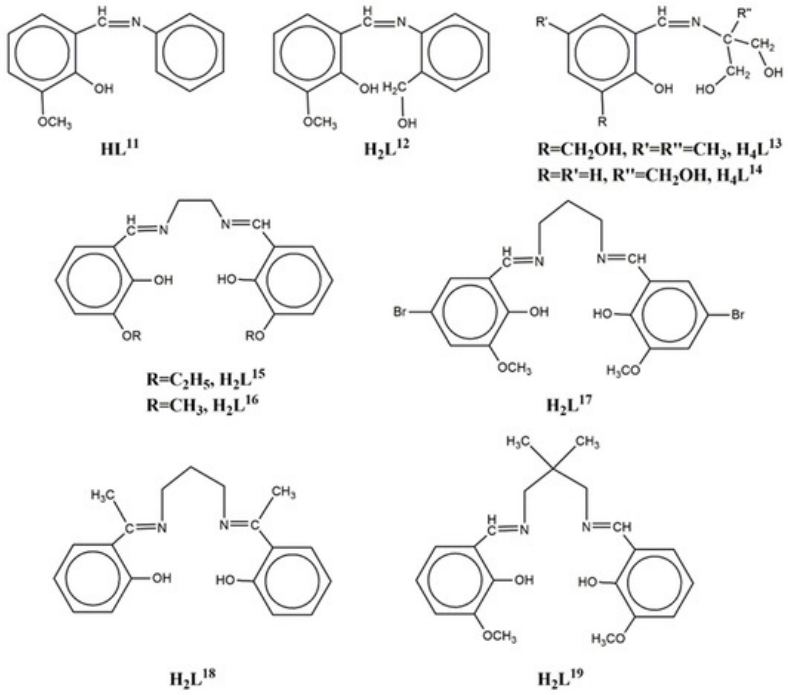

Scheme 2. The Schiff base ligands used in Ni_2Ln complexes **71**–**93**.

The Schiff base ligand H_2L^{12} = (*Z*)-2-(((2-(hydroxymethyl)phenyl)imino)methyl)-6-methoxyphenol (Scheme 2) gave, among others, the linear trinuclear complex $[\{Ni(HL^{12})_2\}_2La(NO_3)](NO_3)_2$ (**75**) which contains two Ni^{II} ions in distorted octahedral N_2O_4 environment and a central La^{III} ion bound to four phenolato and four methoxy oxygen atoms from four $(HL^{12})^-$ ligands and two oxygen atoms from a chelate nitrate[16]. The coordination geometry around the La^{III} ion is best described as sphenocorona JSPC-10 (CShM = 3.37915). Weak antiferromagnetic exchange between the Ni^{II} ions is found in the complex via the closed shell La^{III} ion. The fit of the $\chi_M T$ data from 150 K to 2 K using a HDVV Hamiltonian yielded parameters J = -0.978 cm^{-1}, g = 2.177, D = 3.133 cm^{-1}.

The pentadentate Schiff base ligand H_4L^{13} = (*Z*)-2-((2-hydroxy-3-(hydroxymethyl)-5-methylbenzylidene)amino)-2-methylpropane-1,3-diol (Scheme 2) was used to prepare a family of isostructural complexes $[\{Ni(H_3L^{13})_2\}_2Ln](NO_3)_3$ (Ln^{III} = Gd, Tb, Dy, Ho, **76**–**79**) with linear metal arrangement (Figure 7)[17]. Each of the terminal Ni^{II} ions is distorted octahedral

in N_2O_4 environment; the four oxygen atoms are derived from two phenolates and two pendant -CH_2OH arms of the two different $(H_3L^{13})^-$ ligands. The two imino nitrogen atoms around Ni are *trans* with respect to each other. The central Ln^{III} ion is coordinated to eight oxygen atoms (four benzyl alcohol groups and four phenolato O-atoms) in square antiprismatic geometry. Each Ni_2Ln complex interacts with four neighboring molecules through the -CH_2OH groups of the ligands and the NO_3^- counteranions, leading to 2D H-bonded network along the *ab* plane. The static magnetic properties of all four complexes showed a predominant ferromagnetic interaction between the metal ions and only the Ni_2Dy complex exhibited frequency dependent tails in the χ''_M *vs T* plots under zero dc field. The magnetic properties of complex **76** were analyzed by using the spin Hamiltonian assuming two equivalent $Ni(O)_2Gd$ bridging halves. The best-fit parameters are J_{ex} = +0.67 cm^{-1}, g = 2.117, D = 4.92 cm^{-1} (R = 7 × 10^{-7}). The magnetocaloric properties of the Ni_2Gd were estimated from the experimental isothermal field-dependent magnetization data yielding $-\Delta S_m$ = 11.85 $Jkg^{-1}K^{-1}$ at 4 K and ΔH = 5 T.

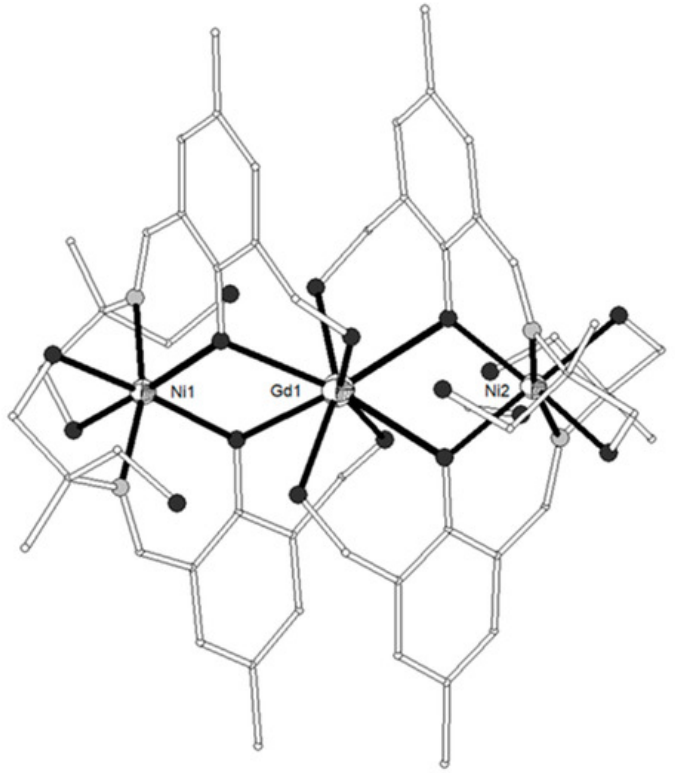

Figure 7. The molecular structure of the cation $[\{Ni(H_3L^{13})_2\}_2Ln]^{3+}$ in complex **76**. Color code as in Figure 2[17].

The Schiff base ligand H_4L^{14} = (*Z*)-2-((2-hydroxybenzylidene)amino)-2-(hydroxymethyl)propane-1,3-diol (Scheme 2) afforded four isostructural complexes with formula $[\{Ni(H_3L^{14})_2\}_2Ln(O_2CMe)_2](NO_3)_3$ (Ln^{III} = Sm, Eu, Gd, Tb, **80**–**83**) with strictly linear metal arrangement (Figure 8)[18]. The two Ni^{II} ions display N_2O_4 distorted octahedral coordination and the central Ln^{III} ion is coordinated to four phenolato oxygen atoms from four $(H_3L^{14})^-$ ligands and four carboxylato oxygen atoms from two chelate acetates describing square antiprismatic geometry. The magnetic susceptibility data of **80** revealed weak antiferromagnetic coupling between the two Ni^{II} ions with best fit parameters J = -0.37 cm^{-1}, g = 1.97 and TIP = 0.001 cm^3mol^{-1}. The $\chi_M T$ product of **81** at 300 K is higher than expected and can be explained by assuming that the first excited states for the Eu^{III} ion are populated at r.t. because they are very close to the ground state. The magnetic susceptibility data of **82** revealed dominant ferromagnetic interactions between the Ni^{II} and Gd^{III} ions and were fitted by using the spin Hamiltonian yielding J_{NiGd} = +0.42 cm^{-1}, D = +2.95 cm^{-1} (g_{Ni} = g_{Gd} = 1.98), resulting in S = 11/2 spin ground state. The magnetocaloric effect of **82** was determined by isothermal magnetization measurements in the temperature range 2–12.5 K under applied magnetic fields up to 5 T with $-\Delta S_m$ = 14.2 $Jkg^{-1}K^{-1}$ at 2 K. The magnetic susceptibility data for **83** are consistent with dominant antiferromagnetic interactions between the metal ions and/or thermal depopulation of the Tb^{III} excited states.

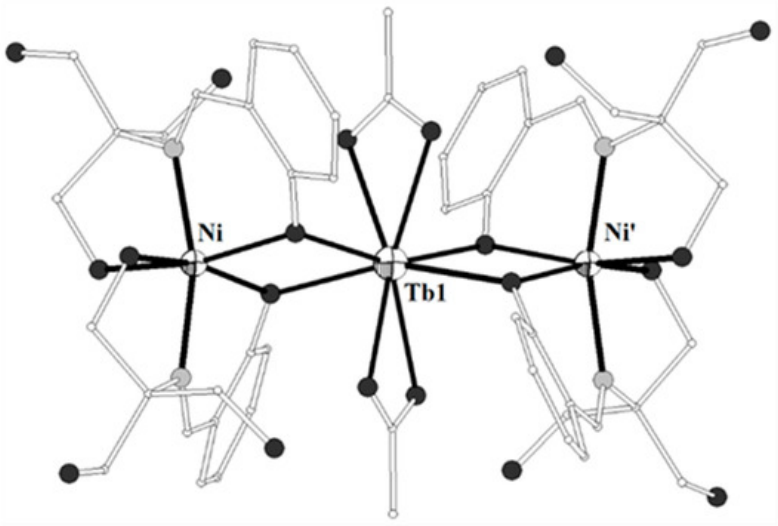

Figure 8. The molecular structure of the cation $[\{Ni(H_3L^{14})_2\}_2Ln(O_2CMe)_2]^+$ in complex **83**. Primed atoms are generated by symmetry: (‘) 1.5-*x*, 0.5-*y*, *z*. Color code as in Figure 2[18].

The hexadentate Schiff base ligand H_2L^{15} = 6,6’-((1*E*,1’*E*)-(ethane-1,2-diylbis(azanylylidene))bis(methanylylidene))bis(2-ethoxyphenol) (Scheme 2) gave two isostructural trinuclear complexes $[(NiL^{15})_2Ln(NO_3)_2](NO_3)$ (Ln^{III} = La, Ce, **84**–**85**) with bent Ni-Ln-Ni arrangement[19]. The central Ln^{III} ion is bound to four phenolato and four ethoxy oxygen atoms as well as to two chelate NO_3^- anions in distorted icosahedron geometry. Each of the terminal Ni^{II} ions is coordinated to the two imino nitrogen and two phenolato oxygen atoms of the ligand in square planar geometry. The Ln^{III} ion is bridged to each of the Ni^{II} ions via two phenolato and two ethoxy oxygen atoms. Both complexes showed antimicrobial activity on cultures of *E.coli*, *S.aureus* and CA. The congener ligand H_2L^{16} (Scheme 2) gave a similar Ni_2Ce complex with Ni-Ce-Ni angle of ~62°[20].

The ligand H_2L^{17} = 6,6’-((1*E*,1’*E*)-(propane-1,3-diylbis(azanylylidene))bis (methanylylidene))bis(4-bromo-2-methoxyphenol) (Scheme 2) gave four isostructural trinuclear complexes $[(NiL^{17})_2Ln(O_2CMe)_2(MeOH)_2](NO_3)$ (Ln^{III} = La, Nd, Ce, Pr, **87**–**90**)[21][22] which contain a central Ln^{III} ion in an inversion center bound to four phenolato and four methoxy oxygen atoms as well as to two acetato oxygen atoms from two carboxylato ligands in pentagonal antiprismatic geometry (Figure 9). Each Ni^{II} ion occupies the N_2O_2 compartment of the ligand and has distorted octahedral geometry with MeOH and bridging acetato oxygen atoms in the apical positions. The Ln^{III} ion is bridged to each of the Ni^{II} ions via the two phenolato oxygen atoms and the acetato group. Weak antiferromagnetic coupling between the Ni^{II} ions through the diamagnetic La^{III} ion was found in the Ni_2La complex **87**. The magnetic susceptibility data were interpreted based on the isotropic Heisenberg model (and the best least-squares fit yielded J = -0.75 cm^{-1}, g = 2.18. The susceptibility data of the Ni_2Nd, Ni_2Ce and Ni_2Pr complexes **88**, **89**, **90** respectively obey the Curie-Weiss law with the Curie constant of C = 3.71 cm^3 K mol^{-1} and the Weiss constant of θ = -7.4 K for **88**, C = 3.23 cm^3 K mol^{-1} and θ = -9.9 K for **89** and C = 4.05 cm^3 K mol^{-1} and θ= -25.5 K for **90**. The negative values of Weiss constant confirm the antiferromagnetic exchange coupling between the metal ions. For complexes **89** and **90**, the crystal field parameters for the Ce^{III}/Pr^{III} ions and the exchange coupling constant were estimated by using the generalized van Vleck formalism. The best fit yielded J_{NiCe} = -1.1(4) cm^{-1}, g_{Ni} = 2.23(3), D = 6.3(4) cm^{-1}, $A^0_2\langle r^2\rangle$ = -265(10) cm^{-1}, $A^0_4\langle r^4\rangle$ = 291(6) cm^{-1} for **89** and J_{NiPr} = -1.3(8) cm^{-1}, g_{Ni} = 2.15(2), D = 7.1(4) cm^{-1}, $A^0_2\langle r^2\rangle$ = -310(9) cm^{-1}, $A^0_4\langle r^4\rangle$ = 2335(11) cm^{-1}, $A^0_6\langle r^6\rangle$ = 80(8) cm^{-1} for **90.**

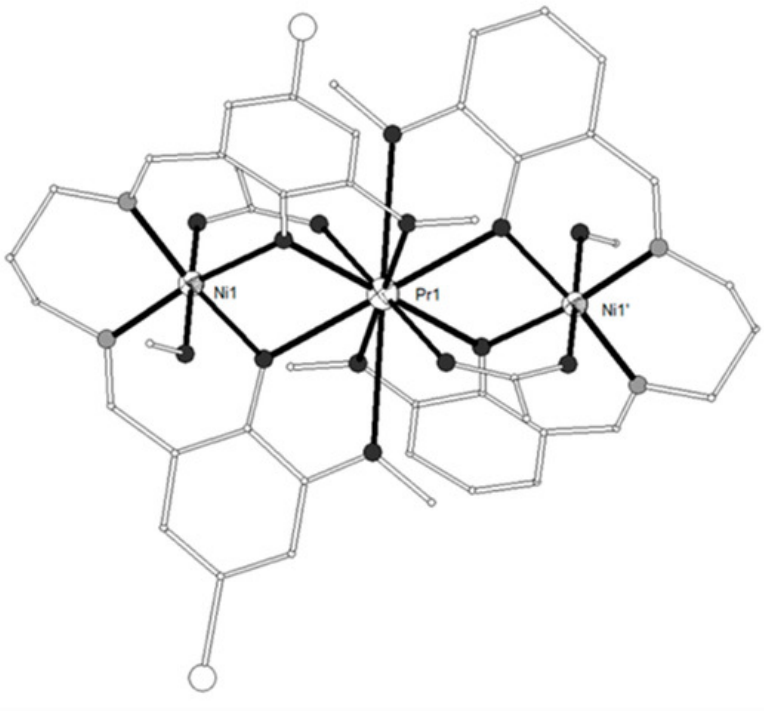

Figure 9. The molecular structure of the cation $[(NiL^{17})_2Pr(O_2CMe)_2(MeOH)_2]^+$ in complex **90**. Primed atoms are generated by symmetry: (') 1-*x*, 1-*y*, 1-*z*. Color code: Gd large octant, Ni small octant, N light grey, O dark grey, C open small, Br open large[22].

The tetradentate Schiff base ligand H_2L^{18} = 2,2'-((1*E*,1'*E*)-(propane-1,3-diylbis (azanylylidene))bis(ethan-1-yl-1-ylidene))diphenol (Scheme 2) gave a trinuclear complex $[(NiL^{18})_2Ce(NO_3)_3]$ (**91**) with a central Ce^{III} ion bound to two terminal $[Ni(L^{18})]$ metalloligands in a *transoid* orientation to the central lanthanide ion[23]. The Ce^{III} ion is ten-coordinate to four phenolato oxygen atoms and to three chelate nitrates, the coordination polyhedron can be described as distorted tetradecahedron. Each Ni^{II} ion is in N_2O_2 square planar geometry. The Ni-Ce-Ni moiety is bent with angle ~122.5°.

The ligand H_2L^{19} = 6,6'-((1*E*,1'*E*)-((2,2-dimethylpropane-1,3-diyl)bis(azanyl ylidene))bis(methanyl ylidene))bis(2-methoxyphenol) (Scheme 2) gave the trinuclear complexes $[\{NiL^{19}(H_2O)\}_2Ln(H_2O)](trif)_3$ (Ln^{III} = Gd, Eu, **92**–**93**; trif = triflate anion) which contain a nine-coordinate central Ln^{III} ion bound to four phenolato and four methoxy oxygen atoms from two $(L^{19})^{2-}$ ligands and a water molecule (Figure 10)[5][24]. Each of the terminal Ni^{II} ions is five-coordinate, linked to the N_2O_2 site of the ligand in the equatorial plane and to a water molecule in the apical position. The magnetic susceptibility data of **92** were fitted considering two different *J* parameters for the Ni-Gd magnetic exchange and an equivalent *D* term for both nickel ions, according to the spin Hamiltonian . The best fit yielded J_{NiGd} = 4.8(3) cm^{-1}, j_{NiGd} = 0.05(2) cm^{-1}, g = 2.03(1) and D = 0.03(1) cm^{-1} ($R = 1 \times 10^{-5}$). A very similar *J* value (0.5 cm^{-1}) yielded when the data were fitted without *j* and *D* parameters. The observed magnetization of 9.3 *Nβ* at 5 T was explained considering a ferromagnetic Ni-Gd dinuclear unit plus a mononuclear pentacoordinate Ni ion having a large magnetic anisotropy due to zero field splitting. The magnetization curve was fitted with J = 5 cm^{-1}, j = 0, D = 12.4 cm^{-1}, g_{Ni} = 2.16 and g_{Gd} = 2.00. The magnetic susceptibility data of **93** is governed by at least two magnetic phenomena that is, the depopulation of the Stark levels of the Eu^{III} ion and the zero-field splitting of the Ni^{II} ions at very low temperatures.

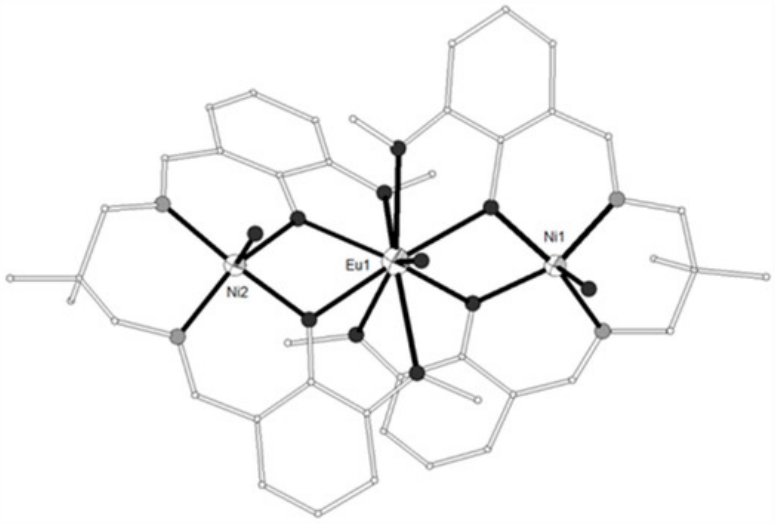

Figure 10. The molecular structure of the cation $[\{NiL^{19}(H_2O)\}_2Eu(H_2O)]^{3+}$ in complex **93**. Color code as in Figure 2[24].

3. Miscellaneous Ligands

The dipodal Schiff base ligand H_4L^{20} = 3,3'-((1*E*,1'*E*)-((((2-aminoethyl)azanediyl)bis(ethane-2,1-diyl))bis(azanylylidene))bis(methanylylidene)) bis(2-hydroxybenzoic acid) (Scheme 3) gave a family of isomorphous V-shaped trinuclear complexes, $[\{Ni(H_2L^{20})(tren)_2\}_2Ln](NO_3)_3$ [Ln^{III} = Gd, Dy, Er, Lu, **94**–**97**; tren = tris(2-aminoethyl)-amine) [25]. The ligand was prepared in situ and this fact justifies the complexation of tren around the Ni^{II} ions (Figure 11). The Ln^{III} ions are eight-coordinate by four phenolato and four carboxylato oxygen atoms from two different ligands in distorted square antiprismatic geometry. Each of the terminal Ni^{II} ions is bound to four nitrogen atoms from the tren ligand, one amino group and one carboxylato oxygen atom from the Schiff base ligand in distorted octahedral geometry. Magnetic studies on all four complexes suggest the presence of weak antiferromagnetic interactions between neighboring ions. The magnetic susceptibility data of the Ni_2Gd complex **94** were interpreted considering the spin Hamiltonian . The best set of parameters obtained using this model is J/k_B = -0.083 cm^{-1} and g = 2.03. In complex **97**, the two Ni^{II} ions are linked by the diamagnetic Lu^{III} ion and the magnetic susceptibility data were interpreted using the spin Hamiltonian considering the axial single-ion zero-field splitting of the two Ni^{II} ions. The data were correctly fitted with D = 3.2(0) K and g = 2.19(2). The fit of the magnetic susceptibility data for **95** and **96** in the range 50–300 K to the Curie-Weiss law gave Curie constant C of 16.19 and 14.42 cm^3 K mol^{-1} and Weiss temperature θ of -4.2 and -7.9 K for **95** and **96** respectively. The negative θ value indicates the presence of antiferromagnetic interactions within the Ni^{II}-Ln^{III}-Ni^{II} moiety.

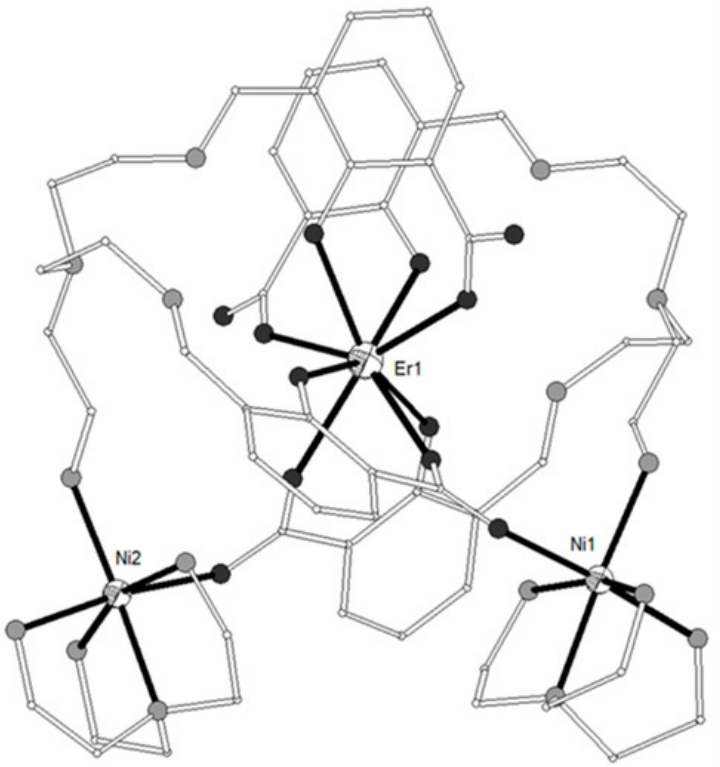

Figure 11. The molecular structure of the cation $[\{Ni(H_2L^{20})(tren)_2\}_2Er]^{3+}$ in complex **96**. Color code as in Figure 2[25].

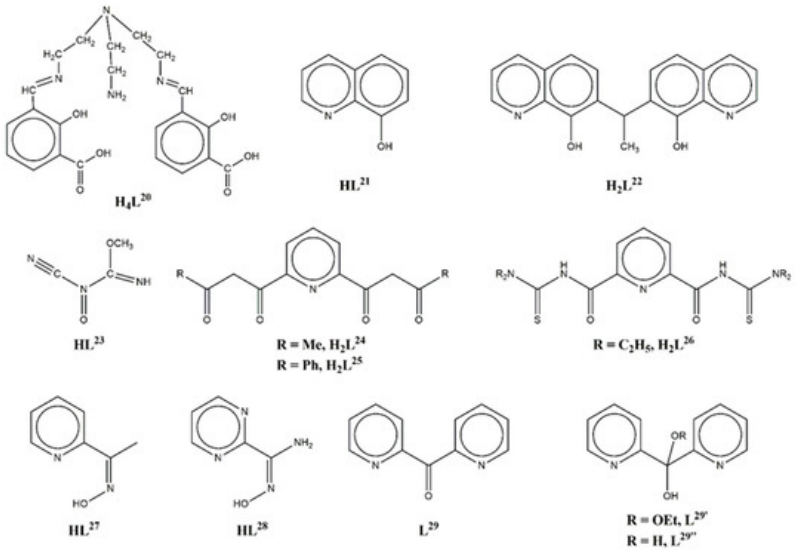

Scheme 3. The ligands used in the Ni_2Ln complexes **94**–**145**.

The ligand 8-hydroxyquinoline, HL^{21} (Scheme 3) gave the trinuclear complex $[\{Ni(L^{21})_3\}_2La(L^{21})]$, **98**[26]. The two Ni^{II} ions are six-coordinate with distorted *fac*-octahedral coordination geometry derived from three chelating $(L^{21})^-$ ligands (O,N). The La^{III} ion is eight-coordinate with distorted square antiprismatic geometry bound to six bridging oxygen atoms of six $(L^{21})^-$ ligands and to a chelate $(L^{21})^-$ ligand through the nitrogen and oxygen atoms. The three metal ions form an angle of ~130°.

The ligand H_2L^{22} = 7,7'-(ethane-1,1-diyl)bis(quinolin-8-ol) (Scheme 3) was formed in situ under the solvo(hydro)thermal conditions used to prepare complexes $[\{Ni(L^{22})_{1.5}\}_2Ln(OH)]$ (Ln^{III} = Eu, Tb, Gd, **99**–**101**) from 8-hydroxyquinoline as proligand[27]. All complexes are isomorphous and crystallize in the hexagonal space group $P6_3/m$. The Ln^{III} ion has position occupation 0.16667 and presents tricapped trigon-prismatic geometry comprised six oxygen atoms from three ligands and three terminal OH^- groups with 0.16667 position occupation. The one crystallographically independent Ni^{II} ion has position occupation 0.33333 and is coordinated to three oxygen and three nitrogen atoms from three ligands creating a regular trigon-antiprismatic geometry. Supramolecular C-H···π interactions between neighboring molecules result in an overall 3D net. The dc susceptibility studies of the Ni_2Tb complex **100** displayed paramagnetic behavior in the temperature range 300–12.5 K and below that temperature a slow decrease in the $\chi_M T$ product mainly due to the thermal depopulation of crystal field effect.

The ligand HL^{23} (Scheme 3) was formed in situ via transition metal promoted nucleophilic addition of methanol to a nitrile group of dicyanonitrosomethanide (dcnm) and gave two families of trinuclear complexes, $(Me_4N)[\{(Ni(L^{23})_3\}_2Ln(L^{23})_2]$ (Ln^{III} = La, Ce, Pr, Nd, Sm, **102**–**106**) and $(Et_4N)_2[\{(Ni(L^{23})_3\}_2Ln(dcnm)_2](ClO_4)$ (Ln^{III} = La, Ce, **107**–**108**)[28]. The two Ni^{II} octahedral metal sites are each coordinated by three $(L^{23})^-$ ligands which chelate through the nitrogen atoms of the nitroso and imine groups to form a $[Ni(L^{23})_3]^-$ metalloligand. The central Ln^{III} ion is bound to two $[Ni(L^{23})_3]^-$ metalloligands and presents ten-coordination completed by two $(L^{23})^-$ ligands or two unreacted $dcnm^-$ ligands, all of them bound via the N,O atoms of the nitroso group (Figure 12). The coordination geometry around the Ln^{III} ions is best described as sphenocorona JSPC-10. The Ni_2Ln moiety is bent in both type of complexes with Ni-Ln-Ni angle of ~142 and ~133° for $(Me_4N)[\{(Ni(L^{23})_3\}_2Ln(L^{23})_2]$ and $(Et_4N)_2[\{(Ni(L^{23})_3\}_2Ln(dcnm)_2](ClO_4)$ complexes, respectively. Variable temperature magnetic susceptibilities on these complexes revealed practically zero Ni-Ni exchange coupling in the Ni_2La complexes **102** and **107**, possible weak antiferromagnetic coupling in Ni_2Pr **104** and possible weak ferromagnetic coupling in the Ni_2Ce complexes **103** and **108** but thermal depopulation and ligand-filed effects on the central Ln^{III} ion, particularly for Sm^{III}, make the unambiguous assignment of ferro- versus antiferromagnetic coupling rather difficult. In any case the magnetic behavior of **102**–**108** is similar to those of congener complexes.

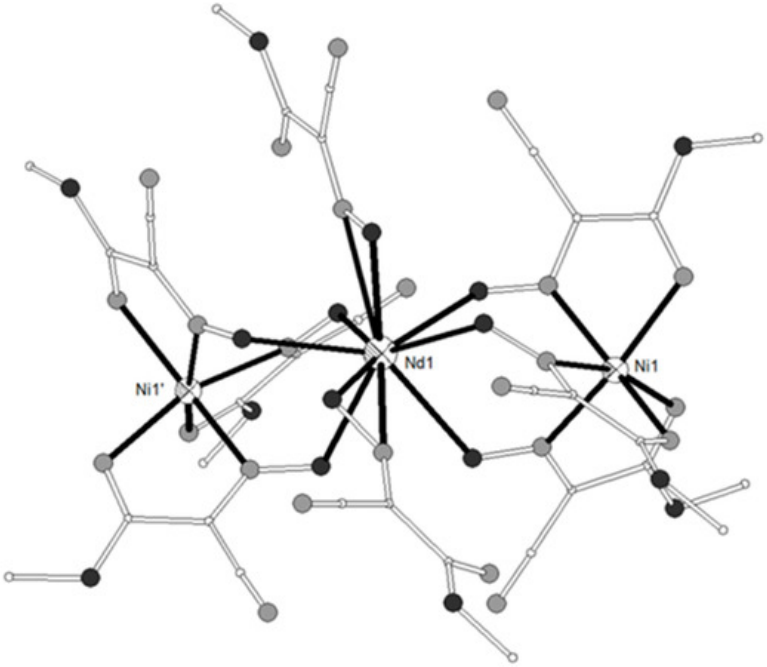

Figure 12. The molecular structure of the anion $[\{(Ni(L^{23})_3\}_2Nd(L^{23})_2]^-$ in complex **105**. Primed atoms are generated by symmetry: (') 1/3 + *y*, -1/3 + *x*, 1/6-*z*. Color code as in Figure 2 [28].

The ligand 2,6-di(acetoacetyl)pyridine, H_2L^{24} (Scheme 3) gave 18 trinuclear $Ni^{II}_2Ln^{III}$ complexes with Ln^{III} = La-Lu except for Pm, which crystallize in four different types: (A) $[(NiL^{24})_2Ln(NO_3)_2(MeOH)_4](NO_3)$ (Ln^{III} = La, Ce, Pr, Nd, Sm, Eu, Gd, **109**–**115**), (B) $[(NiL^{24})_2Ln(NO_3)_2(H_2O)_2(MeOH)_2](NO_3)$ (Ln^{III} = Sm, Eu, Gd, **116**–**118**), (C) $[(NiL^{24})_2Ln(NO_3)_3(MeOH)_4]$ (Ln^{III} = Gd, Tb, Dy, **119**–**121**) and (D) $[(NiL^{24})_2Ln(NO_3)_2(H_2O)(MeOH)_3](NO_3)$ (Ln^{III} = Ho, Er, Tm, Yb, Lu, **122**–**126**)[29]. All types of complexes are linear with Ni-Ln-Ni angles 180° (A), ~178° (B), ~173° (C) and ~179° (D). The two terminal Ni^{II} ions present O_6 distorted octahedral geometry bound to the 1,3-diketonate sites from two $(L^{24})^{2-}$ ligands together with MeOH and H_2O molecules. The central Ln^{III} ion is coordinated to the 2,6-diacylpyridine site from two $(L^{24})^{2-}$ ligands and to two or three nitrate ions in an overall ten-coordinate environment (Figure 13). The coordination geometry around the Ln^{III} ions is best described as hexadecahedron HD-10 in **109**–**115** and tetradecahedron TD-10 in **116**–**126**. The magnetic studies revealed that the Ni-Ln interaction is weakly antiferromagnetic for Ln = Ce, Pr, Nd and ferromagnetic for Ln = Gd, Tb, Dy, Ho, Er. The magnetic susceptibility data for **109** and **126** which contain the diamagnetic La^{III} and Lu^{III} ions, respectively, were interpreted based on the isotropic Heisenberg model . The best-fit parameters are J = -0.63 cm^{-1}, g = 2.22 for **109** and J = -0.65 cm^{-1}, g = 2.17 for **126**. For the Ni_2Gd complex, the spin Hamiltonian (J is the exchange integral between the adjacent Ni^{II} and Gd^{III} ions and J' is the exchange integral between the terminal Ni^{II} ions) was used to fit the susceptibility data and considering g_{Ni} = 2.20 and J' = -0.64 cm^{-1} (the mean values for **109** and **126**) the best-fit parameters are J = +0.79 cm^{-1} g_{Gd} = 2.02. The magnetic data of the remaining complexes were evaluated by adopting an empirical method taking into account the behavior of the congener Zn_2Ln and Ni_2La complexes by using the equation , for ferromagnetic and for antiferromagnetic interaction.

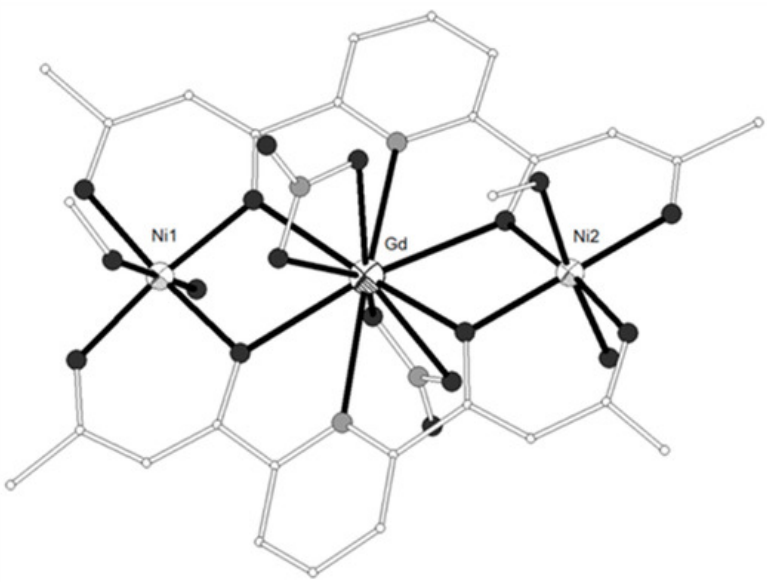

Figure 13. The molecular structure of the cation $[(NiL^{24})_2Gd(NO_3)_2(H_2O)_2(MeOH)_2]^+$ in complex **118**. Color code as in Figure 2[27].

The congener ligand 2,6-bis(acetobenzoyl)pyridine H_2L^{25} (Scheme 3) gave the trinuclear complexes $[(NiL^{25})_2Ln(O_2CMe)_3(MeOH)_x]$ (Ln^{III} = Gd, Ce; x = 2 or 3, **127**–**128**) and $[(NiL^{25})_2Ln(O_2CPh)_3(solv)_x]$ (Ln^{III} = Gd, solv = MeOH, x = 2, **129**; Ce, solv = MeOH/H_2O x = 2, **130**)[30]. Each $(L^{25})^{2-}$ ligand is bound to the Ni^{II} sites through the 1,3-diketonate sites and to the central Ln^{III} ion through the 2,6-diacylpyridine site. Two carboxylato ligands act as bidentate bridging between the Ni^{II} and the Ln^{III} ions and the third act as chelate bidentate around the central lanthanide ion. The six-coordination around the Ni^{II} ions is completed by solvate molecules. The coordination number around the Ce^{III} ion is 10, whereas for the Gd^{III} is 9 or 10. The N_2O_7 nine-coordination around Gd^{III} in **127** is described as HH-9 (hula-hoop) and the N_2O_8 ten-coordination around the Ln^{III} ions in **128**–**130** is described as staggered dodecahedron SDD-10.

The ligand 2,6-dipicolinoylbis(N,N-diethylthiourea) H_2L^{26} (Scheme 3) gave the trinuclear complex $[(NiL^{26})_2Pr(O_2CMe)_3(MeOH)_2]$, **131**[31] [47]. The two Ni^{II} ions are bound to the S,O atoms from two $(L^{26})^{2-}$ ligands, one oxygen atom from the bridging acetato ligand and one methanol in distorted octahedral geometry. The Pr^{III} ion is ten-coordinate and is bound to the O,N,O group of the 2,6-diacylpyridine site of each $(L^{26})^{2-}$ ligand, two bridging and one chelate acetato groups. The polyhedron around the Pr^{III} ion is described as double-capped square antiprism.

The neutral trinuclear complexes $[\{Ni(piv)_3(bpy)\}_2Ln(NO_3)]\cdot MeCN$ (Hpiv = pivalic acid, bpy = 2,2'-bipyridine, Ln^{III} = Gd (**132**), Sm (**133**)) are isomorphous and contain a bent Ni-Ln-Ni moiety with angles ~153°[32]. The central Ln^{III} ion is bound to each of the terminal Ni^{II} ions through two *syn*,*syn* pivalato groups and one μ-O carboxylato oxygen which belongs to a chelate-monodentate bridging pivalato group. The distorted octahedral coordination around each Ni^{II} ion consists of four carboxylato oxygen atoms and two nitrogen atoms of the bpy. The magnetic susceptibility data of **132** were interpreted by using the spin Hamiltonian . The best fit yielded J_{NiGd} = 0.105(5) cm^{-1}, J_{NiNi} = -0.70(5) cm^{-1}, g_{Ni} = 2.015(1), g_{Gd} = 2.00 (fixed), tip = 0.0001 ($R^2 = 1.28 \times 10^{-5}$). The neutral trinuclear complexes $[\{Ni(piv)_3(Hpiv)(MeCN)\}_2Ln(NO_3)]$ (Ln^{III} = La, Pr, Sm, Eu, Gd, **134**–**138**)[32] are isomorphous and contain a Ni-Ln-Ni moiety with angles ~144°. The central Ln^{III} ion is bound to each of the terminal Ni^{II} ions in similar fashion as in **134**–**138**. The coordination of each Ni^{II} ion is completed by a monodentate Hpiv and MeCN molecules and is distorted octahedral. The coordination of the central Ln^{III} consists of six carboxylato oxygen atoms and one chelate nitrato group and is described as single-capped pentagonal bipyramid. The magnetic susceptibility data of **138** were interpreted by using the spin Hamiltonian . The best fit yielded J_{NiGd} = 0.44(2) cm^{-1}, J_{NiNi} = -2.25(5) cm^{-1}, $g_{Ni} = g_{Gd}$ = 2.00 (fixed), molar content of the S = 1 impurity is 5.5% ($R^2 = 1.5 \times 10^{-4}$). The magnetic susceptibility data of **134** can be interpreted by using either the exchange Hamiltonian which yields J_{ex} = -1.0(3) cm^{-1}, g = 2.24(1) and zJ' = +0.9(1) cm^{-1}, tip = 2.4(9) × 10^{-4} ($R^2 = 2.6 \times 10^{-4}$) or by considering the zero-field splitting of the Ni^{II} ions which yields D = 6.0(5) cm^{-1}, g = 2.227(1), zJ' = +0.05(1) cm^{-1}, tip = 3.6(5) × 10^{-4} ($R^2 = 2.5 \times 10^{-3}$). The magnetic susceptibility data for **135–137** which contain Pr^{III}, Sm^{III} and Eu^{III} ions can be interpreted by assuming that the exchange interactions between Ni^{II} and Ln^{III} ions are absent, whereas the weak antiferromagnetic interactions between the Ni^{II} ions 'through the lanthanide' do exist.

The ligands HL^{27} = (*Z*)-1-(pyridine-2-yl)ethenone oxime and HL^{28} = (*E*)-*N*'-hydroxypyrimidine-2-carboximidamide (Scheme 3) gave the trinuclear complexes $[\{Ni(L^{27})_3\}_2Tb](NO_3)$ (**139**)[33][34] and $[(Ni(HL^{28})_3\}_2Tb](NO_3)$ (**140**)[35], respectively. Both complexes contain strictly linear Ni-Tb-Ni moiety (Figures 14). Each of the terminal Ni^{II} ions in **139**–**140** is coordinated to three pyridine and three oximato nitrogen atoms from three $(HL^{27})^-$ or $(HL^{28})^-$ ligands in distorted octahedral geometry. The central Tb^{III} ion is coordinated to six oximato oxygen atoms from the three $(HL^{27})^-$ or $(HL^{28})^-$ ligands (Scheme 3) in distorted octahedral geometry. The $\chi_M T$ values of **139** at 300 and 2 K are 13.54 and 2.80 cm^3 K mol^{-1}, respectively. The field dependence of the magnetization at 2 K is 6.41 $N\mu_B$ at 2 K. The $\chi_M T$ value of **140** at 300 K is 11.74 cm^3 K mol^{-1} which is slightly low with respect to the expected value for two Ni^{II} (S = 1) and one Tb^{III} (S = 3, L = 3, g = 3/2) non-interacting ions. The $\chi_M T$ value decreases on lowering the temperature and reaches the value of 5.41 cm^3 K mol^{-1} at 5 K. The decrease of the $\chi_M T$ value as the temperature decreases for **139** and **140** is governed by the thermal depopulation of the ground-state sublevels as result of the spin-orbit coupling and the low symmetry crystal field.

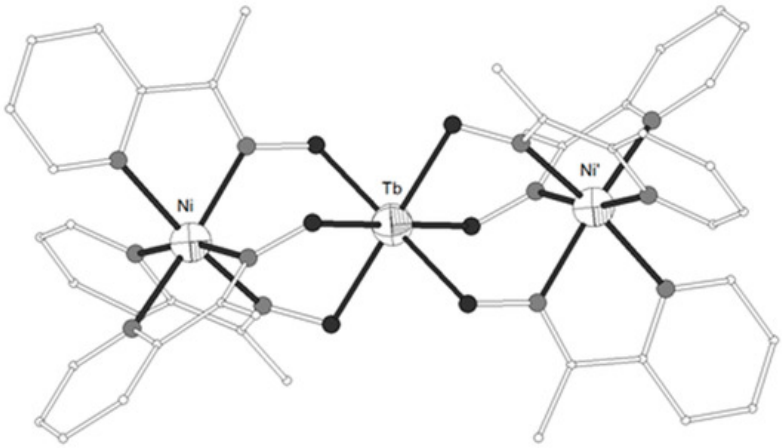

Figure 14. The molecular structure of the cation complex $[\{Ni(L^{27})_3\}_2Tb]^+$ **139**. Primed atoms are generated by symmetry: (') *-x+y*, *-x*, *z*. Color code: Tb large octant, Ni small octant, N light grey, O dark grey, C open small, S open large[34].

It is well known that ligand L^{29} = di(pyridine-2-yl)methanone or di-2-pyridyl ketone (Scheme 3) can undergo nucleophilic addition on the carbonyl carbon atom to form the hemiketal and/or the *gem*-diol ligands $L^{29'}$ = ethoxydi(pyridine-2-yl)methanol and $L^{29''}$ = di(pyridin-2-yl)methanediol, respectively. Both $L^{29'}$ and $L^{29''}$ are formed in situ in the presence of metal ions. Complexes $[Ni_2(L^{29'})_3(L^{29''})Ln(NO_3)(H_2O)](ClO_4)_2$ (Ln^{III} = Gd **141**, Tb **142**) and $[Ni_2(L^{29'})_4Ln(NO_3)(H_2O)][Ln(NO_3)_5](ClO_4)_2$ (Ln^{III} = Tb **143**, Dy **144**, Y **145**) consist of dications which contain triangular Ni-Ln-Ni moieties with angles ~54° (Figure 15)[36][37]. The metal ions are linked through one μ_3-O atom and three μ_2-O atoms from the ligands (Scheme 3). Each Ni^{II} ion is coordinated to three oxygen and two nitrogen atoms from three respective ligands in distorted octahedron. Each Ln^{III} ion is coordinated to N_2O_6 chromophore which consists of three carbonyl O-atoms, three pyridine N-atoms, one chelate nitrato and one terminal aqua ligands. The magnetic susceptibility data of **141** revealed $\chi_M T$ values of 12.61 and 18.63 $cm^3\ K\ mol^{-1}$ at 300 and 2 K respectively. The data were interpreted by using the spin Hamiltonian and the best fit yielded J = +1.03(8) cm^{-1}, J' = +0.9(2) cm^{-1}, g = 2.246(1). The magnetization measurement at 2 K revealed saturation under 5 T at 12.9 μ_β, indicative of an S = 11/2 ground state with a g value larger than 2.0. The magnetic data of **143** revealed ferromagnetic exchange interactions between the metal ions. The magnetic susceptibility data of **145** which contains the diamagnetic Y^{III} ion allowed the determination of the magnetic exchange interaction between the Ni^{II} ions according to the above spin Hamiltonian by considering J = 0. The best fit gave J' = +8.0(2) cm^{-1} and g = 2.15(1).

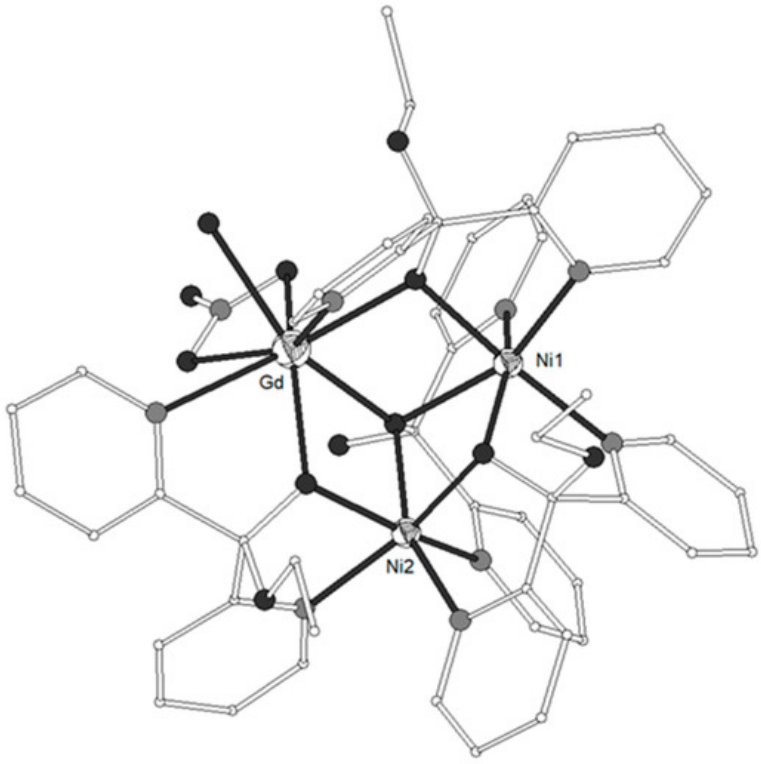

Figure 15. The molecular structure of the dication complex $[Ni_2(L^{29'})_3(L^{29''})Gd(NO_3)(H_2O)]^{2+}$ **141**. Color code: Gd large octant, Ni small octant, N light grey, O dark grey, C open small, S open large[36][37].

The coordination geometry around the Ni^{II} ions in complexes **1**–**145** is distorted octahedral; the only exceptions are complexes **12**–**15** which can be more acutely described as trigonal prismatic. The bridging modes and the coordination around the Ni^{II} ions observed in complexes **1**–**145** is depicted in Scheme 4. The Ni^{II} ions is complexes **1**–**28**, **52**–**74**, **98**–**101** and **141**–**145** are coordinated to three nitrogen and three oxygen atoms. The configuration around the Ni^{II} ions consisting of N_3O_3 coordination sphere is chiral with either a *Δ* or a *Λ* configuration due to the screw coordination arrangement of the achiral tripodal ligands around the metal ion. When two chiral molecules associate, both homochiral (*Δ*-*Δ* or *Λ*-*Λ*) and heterochiral (*Δ*-*Λ*) pairs are possible. Since the above complexes crystallize in centrosymmetric space groups, molecules with *Δ*-*Δ* and *Λ*-*Λ* pairs coexist in the crystals to form racemic crystals. The Ni^{II} ions in complexes **29**–**51**, **75**–**83**, **91**–**93** and **109**–**131** are coordinated to four nitrogen and two oxygen atoms. The Ni^{II} ions in **89**–**90** and **132**–**138** are coordinated to two nitrogen and four oxygen atoms and in **94**–**97** are coordinated to five nitrogen and one oxygen atoms. The Ni^{II} ions in **102**–**108** and **139**–**140** show N_6 coordination sphere. On the other hand, the coordination around the Ln^{III} ions in **1**–**145** displays a variety of geometries from the rare octahedral and quasi trigonal prism for O_6 coordination, capped trigonal prism and capped octahedron for O_7 coordination, square antiprism and bicapped octahedron for O_8 and NO_7 coordination, tricapped trigonal prism for O_9 coordination and distorted icosahedron for O_{12} coordination.

References

1. Chandrasekhar, V.; Pandian, B.M.; Boomishankar, R.; Steiner, A.; Vittal, J.J.; Houri, A.; Clérac, R. Trinuclear heterobimetallic Ni2Ln complexes [L2Ni2Ln](ClO4) (Ln = La, Ce, Pr, Nd, Sm, Eu, Gd, Tb, Dy, Ho, and Er; LH3 = (S)P[N(Me)N=CH-C6H3-2-OH_3-OMe]3): From simple paramagnetic complexes to single-molecule magnet behavior. Inorg. Chem. 2008, 47, 4918–4929.
2. Singh, S.K.; Rajeshkumar, T.; Chandrasekhar, V.; Rajaraman, G. Theoretical studies on {3d-Gd} and {3d-Gd-3d} complexes: Effect of metal substitution on the effective exchange interaction. Polyhedron 2013, 66, 81–86.
3. Yamaguchi, T.; Sunatsuki, Y.; Kojima, M.; Akashi, H.; Tsuchimoto, M.; Re, N.; Osa, S.; Matsumoto, N. Ferromagnetic NiII-GdIII interactions in complexes with NiGd, NiGdNi, and NiGdGdNi cores supported by tripodal ligands. Chem. Commun. 2004, 1048–1049.
4. Yamaguchi, T.; Sunatsuki, Y.; Ishida, H.; Kajima, M.; Akashi, H.; Re, N.; Matsumoto, N.; Pochaba, A.; Mroziński, J. Synthesis, structures, and magnetic properties of double face-sharing heterotrinuclear NiII-LnIII-NiII (Ln = Eu, Gd, Tb, and Dy) complexes. Bull. Chem. Soc. Jpn. 2008, 81, 598–605.
5. Jean-Pierre Costes; Tomoka Yamaguchi; Masaaki Kojima; Laure Vendier; Experimental Evidence for the Participation of 5d GdIIIOrbitals in the Magnetic Interaction in Ni−Gd Complexes. *Inorganic Chemistry* **2009**, *48*, 5555-5561, 10.1021/ic900142h.
6. Min-Xia Yao; Zhao-Xia Zhu; Xing-Yun Lu; Xiao-Wei Deng; Su Jing; Rare single-molecule magnets with six-coordinate Ln III ions exhibiting a trigonal antiprism configuration. *Dalton Transactions* **2016**, *45*, 10689-10695, 10.1039/C6DT01606E.
7. Zhiqiang Xu; Paul W. Read; David E. Hibbs; Michael B. Hursthouse; K. M. Abdul Malik; Brian O. Patrick; Steven J. Rettig; Mehran Seid; David A. Summers; Maren Pink; et al. Coaggregation of paramagnetic d- and f-block metal ions with a podand-framework amine phenol ligand.. *Inorganic Chemistry* **2000**, *39*, 508-516, 10.1021/ic991171b.
8. Bayly, S.R.; Xu, Z.; Patrick, B.O.; Rettig, S.J.; Pink, M.; Thompson, R.C.; Orvig, C. d/f complexes with uniform coordination geometry: Structural and magnetic properties of an LnNi2 core supported by a heptadentate amine phenol ligand. Inorg. Chem. 2003, 42, 1576–1583.
9. Mustapha, A.; Reglinski, J.; Kennedy, A.R. The use of hydrogenated Schiff base ligands in the synthesis of milti-metallic compounds. Inorg. Chim. Acta 2009, 362, 1267–1274.
10. He-Rui Wen; Piao-Ping Dong; Sui-Jun Liu; Jin-Sheng Liao; Fu-Yong Liang; Cai-Ming Liu; 3d–4f heterometallic trinuclear complexes derived from amine-phenol tripodal ligands exhibiting magnetic and luminescent properties. *Dalton Transactions* **2017**, *46*, 1153-1162, 10.1039/c6dt04027f.
11. Cheri A. Barta; Simon R. Bayly; Paul W. Read; Brian O. Patrick; Robert C. Thompson; Chris Orvig; Molecular Architectures for Trimetallic d/f/d Complexes: Structural and Magnetic Properties of a LnNi2Core. *Inorganic Chemistry* **2008**, *47*, 2280-2293, 10.1021/ic701612e.
12. Peter Comba; Markus Enders; Michael Großhauser; Markus Hiller; Dennis Müller; Hubert Wadepohl; Solution and solid state structures and magnetism of a series of linear trinuclear compounds with a hexacoordinate Ln III and two terminal Ni II centers. *Dalton Transactions* **2017**, *46*, 138-149, 10.1039/C6DT03488H.

13. He-Rui Wen; Jia-Li Zhang; Fu-Yong Liang; Kai Yang; Sui-Jun Liu; Jinsheng Liao; Cai-Ming Liu; TbIII/3d–TbIII clusters derived from a 1,4,7-triazacyclononane-based hexadentate ligand with field-induced slow magnetic relaxation and oxygen-sensitive luminescence. *New Journal of Chemistry* **2019**, *43*, 4067-4074, 10.1039/c8nj05777j.

14. Upadhyay, A.; Komatireddy, N.; Ghirri, A.; Tuna, F.; Langley, S.K.; Srivastava, A.K.; Sañudo, E.C.; Moubaraki, B.; Murray, K.S.; McInnes, E.J.L.; et al. Synthesis and magnetothermal properties of a ferromagnetically coupled NiII-GdIII-NiII cluster. Dalton Trans. 2014, 43, 259–266.

15. Upadhyay, A.; Das, C.; Langley, S.K.; Murray, K.S.; Srivastava, A.K.; Shanmugam, M. Heteronuclear Ni(II)-Ln(III) (Ln = La, Pr, Tb, Dy) complexes: Synthesis and single-molecule magnet behavior. Dalton Trans. 2016, 45, 3616–3626.

16. Ahmed, N.; Das, C.; Vaidya, S.; Kumar Srivastava, A.; Langley, S.K.; Murray, K.S.; Shanmugam, M. Probing the magnetic and magnetothermal properties of M(II)-Ln(III) complexes (where M(II) = Ni or Zn; Ln(III) = La or Pr or Gd). Dalton Trans. 2014, 43, 17375–17384.

17. Das, S.; Dey, A.; Kundu, S.; Biswas, S.; Mota, A.J.; Colacio, E.; Chandrasekhar, V. Linear {NiII-LnIII-NiII} complexes containing twisted planar Ni(μ-phenolate)2Ln fragments: Synthesis, structure, and magnetothermal properties. Chem. Asian. J. 2014, 9, 1876–1887.

18. Anastasia N. Georgopoulou; M. Pissas; Vassilis Psycharis; Yiannis Sanakis; Catherine P. Raptopoulou; Trinuclear NiII-LnIII-NiII Complexes with Schiff Base Ligands: Synthesis, Structure, and Magnetic Properties. *Molecules* **2020**, *25*, 2280, 10.3390/molecules25102280.

19. Sui, Y.; Hu, R.-H.; Liu, D.-S.; Wu, Q. Adjustment of the structures and biological activities by the ratio of NiL to RE for two sets of Schiff base complexes [(NiL)nRE] (n = 1 or 2; RE = La or Ce). Inorg. Chem. Comm. 2011, 14, 396–398.

20. Ali Güngör, S.; Kose, M. Synthesis, crystal structure, photoluminescence and electrochemical properties of a sandwiched Ni2Ce complex. J. Mol. Struct. 2017, 1150, 274–278.

21. Cristovao, B.; Kłak, J.; Miroslaw, B. Synthesis, crystal structures and magnetic behavior of NiII-4f-NiII compounds. Polyhedron 2012, 43, 47–54.

22. Cristóvão, B.; Kłak, J.; Pełka, R.; Miroslaw, B.; Hnatejko, Z. Heterometallic trinuclear 3d-4f-3d compounds based on a hexadentate Schiff base ligand. Polyhedron 2014, 68, 180–190.

23. Ghosh, S.; Ghosh, A. Coordination of metalloligand [NiL] (H2L = salen type N2O2 Schiff base ligand) to the f-block elements: Structural elucidation and spectrophotometric investigation. Inorg. Chim. Acta 2016, 442, 64–69.

24. Costes, J.-P.; Donnadieu, B.; Gheorghe, R.; Novitchi, G.; Tuchagues, J.-P.; Vendier, L. Di- or trinuclear 3d-4f Schiff base complexes: The role of anions. Eur. J. Inorg. Chem. 2008, 5235–5244.

25. Bhunia, A.; Yadav, M.; Lan, Y.; Powell, A.K.; Menges, F.; Riehn, C.; Niedner-Schatteburg, G.; Jana, P.P.; Riedel, R.; Harms, K.; et al. Trinuclear nickel-lanthanide compounds. Dalron Trans. 2013, 42, 2445–2450.

26. Deacon, G.B.; Forsyth, C.M.; Junk, P.C.; Leary, S.G. A rare earth alloy as a synthetic reagent: Contrasting homometallic rare earth and heterobimetallic outcomes. New J. Chem. 2006, 30, 592–596.

27. Zhu, Y.; Luo, F.; Song, Y.-M.; Feng, X.-F.; Luo, M.-B.; Liao, Z.-W.; Sun, G.-M.; Tian, X.-Z.; Yuan, Z.-J. The first one-pot synthesis of multinuclear 3d-4f metal-organic compounds involving a polytopic N,O-donor ligand formed in situ. Cryst. Growth Des. 2012, 12, 2158–2161.

28. Chesman, A.S.R.; Turner, D.R.; Moubaraki, B.; Murray, K.S.; Deacon, G.B.; Batten, S.R. Synthesis and magnetic properties of a series of 3d/4f/3d heterometallic trinuclear complexes incorporating in situ ligand formation. Inorg. Chim. Acta 2012, 389, 99–106.

29. Shiga, T.; Ito, N.; Hidaka, A.; Okawa, H.; Kitagawa, S.; Ohba, M. A series of trinuclear CuIILnIIICuII complexes derived from 2,6-di(acetoacetyl)pyridine: Synthesis, structure, and magnetism. Inorg. Chem. 2007, 46, 3492–3501.

30. Trieu, T.N.; Nguyen, M.H.; Abram, U.; Nguyen, H.H. Syntheses and structures of new trinuclear MIILnMII (M = Ni, Co; Ln = Gd, Ce) complexes with 2,6-bis(acetobenzoyl)pyridine. Z. Anorg. Allg. Chem. 2015, 641, 863–870.

31. Nguyen, H.H.; Jegathesh, J.J.; Takiden, A.; Hauenstein, D.; Pham, C.T.; Le, C.D.; Abram, U. 2,6-dipicolinoylbis(N,N-dialkylthioureas) as versatile building blocks for oligo- and polynuclear architectures. Dalton Trans. 2016, 45, 10771–10779.

32. Burkovskaya, N.P.; Orlova, E.V.; Kiskin, M.A.; Efimov, N.N.; Bogomyakov, A.S.; Fedin, M.V.; Kolotilov, S.V.; Minin, V.V.; Aleksandrov, G.G.; Sidorov, A.A.; et al. Synhtesis, structure, and magnetic properties of heterometallic trinuclear complexes {MII-LnIII-MII} (MII = Ni, Cu; LnIII = La, Pr, Sm, Eu, Gd). Russ. Chem. Bull Int. Ed. 2011, 60, 2490–2503.

33. Christina D. Polyzou; Constantinos G. Efthymiou; Albert Escuer; Luís Cunha-Silva; Constantina Papatriantafyllopoulou; Spyros P. Perlepes; In search of 3d/4f-metal single-molecule magnets: Nickel(II)/lanthanide(III) coordination clusters. *Pure and Applied Chemistry* **2013**, *85*, 315-327, 10.1351/pac-con-12-09-08.

34. Constantina Papatriantafyllopoulou; Marta Estrader; Constantinos G. Efthymiou; Despina Dermitzaki; Konstantinos Gkotsis; Aris Terzis; Carmen Díaz; Spyros P. Perlepes; In search for mixed transition metal/lanthanide single-molecule magnets: Synthetic routes to NiII/TbIII and NiII/DyIII clusters featuring a 2-pyridyl oximate ligand. *Polyhedron* **2009**, *28*, 1652-1655, 10.1016/j.poly.2008.10.024.
35. Kalogridis, C.; Palacios, M.A.; Rodríguez-Diéguez, A.; Mota, A.J.; Choquesillo-Lazarte, D.; Brechin, E.K.; Colacio, E. Heterometallic oximato-bridged linear trinuclear NiII-MIII-NiII (MIII = Mn, Fe, Tb) complexes constructed with the fac-O3 [Ni(HL)3]− metalloligand (H2L = pyrimidine-2-carboxamide oxime): A theoretical and experimental magneto-structural study. Eur. J. Inorg. Chem. 2011, 5225–5232.
36. Efthymiou, C.G.; Georgopoulou, A.N.; Papatriantafyllopoulou, C.; Terzis, A.; Raptopoulou, C.P.; Escuer, A.; Perlepes, S.P. Initial employment of di-2-pyridyl ketone as a route to nickel(II)/lanthanide(III) clusters: Triangular Ni2Ln complexes. Dalton Trans. 2010, 29, 8603–8605.
37. Georgopoulou, A.N.; Efthymiou, C.G.; Papatriantafyllopoulou, C.; Psycharis, V.; Raptopoulou, C.P.; Manos, M.; Tasiopoulos, A.J.; Escuer, A.; Perlepes, S.P. Triangular NiII2LnIII and NiII2YIII complexes derived from di-2-pyridyl ketone: Synthesis, structures and magnetic properties. Polyhedron 2011, 30, 2978–2986.
